



Accurate numerical prediction of thermo-mechanical behaviour and phase fractions in SLM components of advanced high strength steels for automotive applications

Kiranmayi Aburri Venkata¹, Rohith Uppaluri¹, Bernd Schob², Camilo Zopp², Richard Kordass³, Jan Bohlen³, Matthias Höfemann⁴, Marcin Kasprowicz⁵, Andrzej Pawlak⁶, Edward Chlebus⁶

- ¹) Simufact engineering gmbh, a Hexagon company, kiranmayi.abburivenkata@hexagon.com, nagasairohith.uppaluri@hexagon.com, Tempowerkring 19, 21079 Hamburg, Germany
- ²) Chemnitz University of Technology, Department of Lightweight Structures and Polymer Technology, bernd.schob@mb.tu-chemnitz.de, camilo.zopp@mb.tu-chemnitz.de, Reichenhainer Straße 31/33, 09126 Chemnitz, Germany
- ³) EDAG Engineering GmbH, CAE and Safety Department, richard.kordass@edag.com, jan.bohlen@edag.com, Robert-Bosch-Straße 7a, 85053 Ingolstadt, Germany
- ⁴) Salzgitter Mannesmann Forschung GmbH, Department Welding and Joining Technology, m.hoefemann@sz.szmf.de, Eisenhüttenstraße 99, 38239 Salzgitter, Germany
- ⁵) Wadim Plast Sp. z o.o., marcin.kasprowicz@wadim.com.pl, Ul. Graniczna 10, 05-816 Reguły, Poland
- ⁶) Centre for Advanced Manufacturing Technologies CAMT, Faculty of Mechanical Engineering, Wrocław University of Science and Technology, andrzej.p.pawlak@pwr.edu.pl, edward.chlebus@pwr.edu.pl, ul. Lukasiewicza 5, 50-371 Wrocław, Poland

Keywords

Advanced High Strength Steels (AHSS), Crash Application, Laser Powder Bed Fusion (L-PBF), Numerical Simulation, Phase Predictions

Abstract

Conventional crash absorber in automotive applications, so called crash boxes are fabricated via deep drawn sheet metal resulting in significant lead times and costs. Laser Powder Bed Fusion processes, like Selective Laser Melting (SLM) offer an attractive alternative for the fabrication of crash parts while eliminating any need for costly forming dies and reducing the lead times, provided required material properties are achieved. Reliable numerical simulation model to predict the SLM build process with greater spatial resolution and accuracy is indispensable to understand the process further in order to ensure its applicability to crash structures. In this paper, an improved simulation methodology for SLM process is presented to predict the material behaviour via temperature, deformation, hardening, flow stress and phase fractions throughout the component with increased accuracy and greater resolution. To achieve desired spatial resolution, the equivalent layers are subdivided into individual tracks, which are then deposited sequentially to simulate the printing process. The material is a medium manganese (7-8 %) transformation induced plasticity (TRIP) steel with austenite and martensite primary phases. The multiple solid-state phase transformation cycles undergone by the material are modelled in the simulation and the final phases are predicted. The results indicate improved accuracy and higher resolution in predictions for temperature, phase fractions and deformation.

1 Introduction

The need for reducing carbon footprint of the automotive industry requires improved fuel efficiency among other things. This requirement has moved the automotive industry in search of advanced materials with high strength, ductility and improved crash resistance. To achieve the desired ease of formability whilst maintaining sufficiently high strength and mechanical properties in service, requires

Digital Object Identifier: <http://dx.doi.org/10.21935/tls.v5i1.145>
www.lightweight-structures.de

This is an open access article under the CC BY 4.0 license (<http://creativecommons.org/licenses/by/4.0/>)

further evolution of advanced high strength steels (AHSS) [1, 2]. AHSS evolved from 1st generation (Gen) to 3rd Gen ranging from dual-phase steels, martensitic steels (1st Gen) to high manganese twinning induced plasticity (TWIP) steels (2nd Gen, 15-22 % Mn) to medium manganese (3rd Gen, 3-10 % Mn). The major advantages of the 3rd Gen medium manganese steels include among others reduced production costs and increased weldability, opening up whole new application possibilities for automotive industry [2].

The automotive crash box is one of the most important components to ensure the safety of the passengers and the vehicle while keeping the repair costs to a minimum, by absorption of energy in the event of a low-speed crash [3]. Usually improvements to the crashworthiness are achieved by either changes to the existing design of the crash box or usage of new material or both [4]. The crash boxes are usually manufactured by extrusion or deep drawing of the material using forming dies to achieve the desired geometry [5]. Therefore, any modification in the design currently requires creation of new forming dies, leading to significantly higher costs and lead times.

Selective Laser Melting (SLM) of metals is an efficient and resource-saving additive manufacturing process (AM) that is quite suitable for prototyping and tooling applications in automotive industry [6, 7]. The design freedom associated with AM along with the elimination of costly forming dies and reduced manufacturing times have the potential to ease the critical bottlenecks in the prototyping phase for crash components. However, the repetitive thermal cycles incurred during the SLM process result in changed material properties (especially for medium manganese steels), which are unfavorable for crash applications. Therefore, suitable microstructure tailoring via appropriate local and global post-processing is mandatory in such applications.

Simulation of SLM processes and the process chain can provide crucial information about the material behaviour and any challenges (such as cracking) during the actual manufacturing [8]. Considerable efforts have been laid in this direction over recent years to simulate the SLM process with greater accuracy and resolution in order to elevate simulation as a Design for Additive Manufacturing (DfAM) tool [8, 9]. In this paper, an improved methodology for the simulation of SLM process is presented for higher accuracy and spatial resolution in the predictions. The methodology is applied for the prediction of the material state in a representative crash geometry, in terms of temperature, phase fractions, stresses/strains, deformation and hardening. Advanced high strength steels such as dual phase steels are favoured as a suitable candidate for crash box applications due to the excellent combination of strength and ductility.

2 Material

The material used in the current paper is an experimental medium manganese steel with the chemical composition indicated in Table 1. To produce prototypes with SLM process a medium-Manganese material powder concept is developed to generate typical properties on crash box material applications taking advantage of TRIP effect. This material and its processing builds on the research from “Ein niedriglegierter Stahlwerkstoff für die Laseradditive Fertigung – Prozesskette und Eigenschaften“ [10]. This is spherical powder with a particle fraction of 20-63 μm . Specimens used in research series were fabricated on EOS M290 (EOS GmbH, Krailling, Germany), which has a build chamber size of 250 x 250 x 325 mm^3 . As energy source, a fibre laser was used with a maximum power of 400 W (cw). The SLM process parameters such as laser power and laser focus were retained constant during the studies. The process environment like platform preheating and O_2 content remain unchanged in all research series. A homogenous layer thickness ($t = 30 \mu\text{m}$) was generated using a coating system with integrated polymer wiper. The SLM process parameters are provided in Table 2.

JMatPro software (V11, Sente Software Ltd., Guildford, UK) was employed in determining temperature dependent thermal, mechanical properties and stress/strain curves to be used in the simulation. Considering the fact that the material has two phases (austenite, martensite), the initial property set has been evaluated with 100% martensite as the total phase.

In addition to thermo-mechanical properties and stress/strain graphs, dilatometry curves are required to simulate the phase transformation behaviour during heating and cooling respectively. This includes the AC1, AC3, Ms and Mf temperatures for phase changes during heating and cooling respectively and also the volume change associated with the austenite to martensite transformation during cooling which were supplied by Salzgitter Mannesman Forschung GmbH through dilatometry studies.

Table 1: Chemical composition of the experimental medium manganese steel

Element	Fe	Mn	Si	Al	P	C	S	O	N	H
(%)	balance	7.5– 8.5	0.4– 0.5	1.7– 2.0	0– 0.05	0.08– 0.15	0– 0.05	0– 0.05	0– 0.03	0– 0.005

3 Simulation methodology

3.1 Equivalent heat flux method

To ensure better accuracy of the SLM process and capture the transient thermal behaviour effectively, without entirely sacrificing computational efficiency, a different scheme of layer deposition than conventional approach is presented. This scheme is different than that of a full layer deposition and is loosely based on [11]. In this deposition scheme, an equivalent layer is divided into several individual tracks and these tracks are then deposited sequentially to simulate the printing process. Such schemes have already been used in Computational Fluid Dynamics (CFD) [12] and thermo-mechanical simulation of Directed Energy Deposition (DED) techniques [13].

In order to increase the computational efficiency, several layers are lumped together first as an equivalent layer which was then subdivided to individual tracks. This way, the transient behaviour within the plane of the current layer is captured. A sensitivity study was conducted to ensure the number of layers that can be lumped together, without affecting the predictions severely. The energy balance is achieved by maintaining the speed of the laser and the track deposition time the same as in the real SLM process but recalculating the equivalent heat flux/power based on the track dimensions. The schematic and the implementation methodology are provided below (see Figure 1).

3.2 Creation of tracks

The creation of the tracks is shown schematically in Figure 1. The layers shown in the figure are several SLM layers lumped together and each of these lumped layers is further divided into tracks. The model is set-up such that each of these tracks in a single lumped layer are laid sequentially to complete a single layer. And then moved to the first trajectory in the second lumped layer.

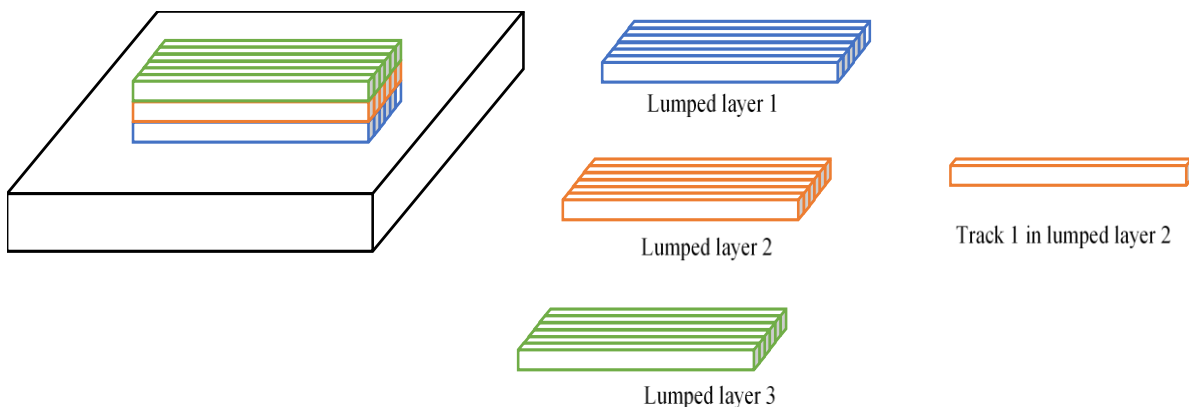


Figure 1: Schematic of lumped layers and tracks

The energy conservation is also achieved by calculating the equivalent power for the track dimensions such that the heat flux remains the same as that of a laser spot heating a single bead/spot. The velocity is maintained the same as in the actual SLM process. The time step for heating the entire track is assigned as the time required to heat a single laser spot at the given velocity. The remaining time difference is assigned as cooling time for each track. To explain this further, consider a laser power of P with a velocity v . The hatch distance is h , the laser spot diameter is d and the layer thickness is t .

If we assume that the laser spot heats a region approximately equal to its diameter, then the time required to heat the spot is t_h given by (1).

$$t_h = \frac{d}{v} \tag{1}$$

Considering the track length (t_l) as the scan length, keeping the velocity the same, the total time for completing the scan length (t_s) is given by (2).

$$t_s = \frac{t_l}{v} \tag{2}$$

However, to guarantee the heat flux to be same, the heating time for the track is taken as t_h and $t_s - t_h$ is considered as the cooling time for the single track. This is similar to assuming several laser spots heating the multiple spots in a trajectory at the same time and same speed. Furthermore, the heat flux (hf_s) for heating a spot is calculated based on the laser spot diameter and the thickness of a single SLM layer as in (3).

$$hf_s = \frac{Pt_h}{dht} \tag{3}$$

Now the equivalent power (P_t) for the track can be calculated by the assumption of equal heat flux as shown in (4).

$$P_t = \frac{P \times \text{volume of the track}}{\text{volume of the laser spot}} \tag{4}$$

A suitable energy expose factor is chosen for appropriate temperature predictions in the melt pool. The current implementation scheme does not consider the influence of rotation of scan vectors as several layers are lumped together combining multiple scan vector rotations.

Table 2: SLM process parameters for double-hat geometry

Laser power (W)	Laser speed (m/s)	Hatch distance (mm)	Layer thickness (mm)	Laser spot diameter (mm)
265	1.0	0.09	0.03	0.1

4 Implementation scheme

4.1 Test geometry

To apply the proposed equivalent heat flux methodology, a representative crash box profile termed as “double-hat” originally used for material characterisation is chosen as a model geometry, shown in Figure 2. The bounding box dimensions of the double-hat are 118 x 79 x 200 mm³ and that of the baseplate are 300 x 300 x 20 mm³ respectively. The double-hat geometry is subdivided into 200 equivalent layers in the build direction. Each layer is further divided into 6 tracks. The elements corresponding to a single track are activated sequentially and the build process is simulated using fully coupled thermo-mechanical simulation.

Based on the equivalent heat flux method explained above, the power required for heating the entire track is calculated, keeping the heating time and the velocity of the robot the same as in the actual SLM process. To increase the accuracy of the predictions in the baseplate, a mesh refinement is used in the baseplate closer to the double-hat and the regions away from the part are meshed with coarser elements. First order hexahedral elements with an approximate size of 1 mm are used for meshing the crash component. In order to facilitate the creation of structured mesh, the holes in the geometry are ignored as these can be later created via a machining simulation.

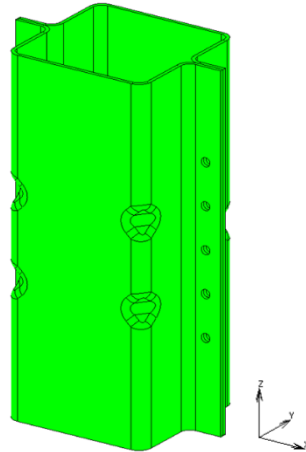


Figure 2: Representative crash box geometry - double-hat profile

4.2 Model set-up

The model is set-up in commercial welding software Simufact Welding 2021 using the dedicated DED module as shown in Figure 3. Considering that the thermal behaviour of the molten material is the major contributor to the subsequent stress/strain and phase generation in the SLM process, which is similar to that of DED fundamentally, the analysis was modelled using DED module for ease of modelling and usage of certain in-built features. The mesh of the part and the baseplate along with the track definitions are shown in Figure 3 (bottom) and 3 (top) respectively. The baseplate is considered as the same material as that of the double-hat and maintained at a temperature of 125 °C during the build process. To avoid rigid body movement, some nodes on the bottom surface of the baseplate are fixed. Temperature dependent thermal, mechanical properties and stress/strain curves generated in section 2 were employed for the thermo-mechanical simulation of the SLM process. Element activation and deactivation is used to mimic the deposition of powder layers sequentially.

Furthermore, in SLM process, the build part is surrounded by powder that acts as a heat insulation and therefore, the heat loss to the surroundings is significantly different than that of a DED process. The simulation has been modified to take this into account by allowing only the top surface of the current layer to contribute to the heat losses. Since the available top surface for heat loss changes dynamically with every new track, this surface is recalculated after every subsequent new track is laid. In order to achieve this constant time stepping scheme was used for the heating process to recalculate the available surface for convection/radiation during SLM build.

The heat loss from the top surface is calculated using a convective heat transfer coefficient of 250 W/m²K and a radiation emissivity of 0.9. The contact heat transfer coefficient between the part and the baseplate is also modelled using a contact heat transfer coefficient of 1000 W/m²K. The entire double-hat profile is considered as a single part with no contact considerations between one layer to another and therefore no contact heat transfer is modelled between individual layers of the double-hat.

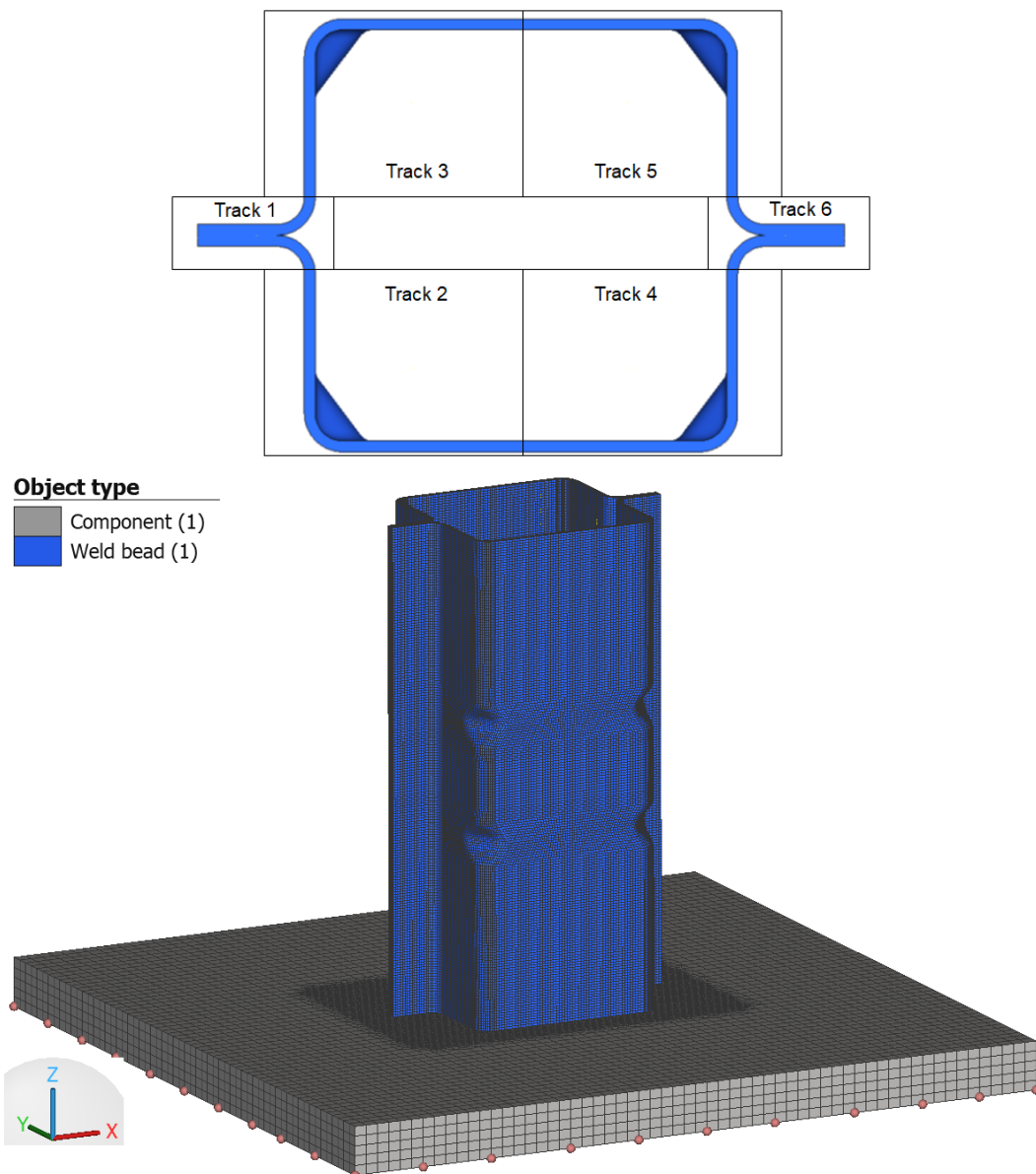


Figure 3: Schematic of the track order (top); Finite Element mesh of the part and the baseplate (bottom)

5 Multi-cycle phase transformation model

During the build process the previously deposited layers will be subjected to multiple thermal cycles, leading to multiple phase transformation or even partial phase transformation during heating from martensite to austenite. Similarly, during cooling down, there can be several cases where the handling of retained austenite requires different approaches. To support the simulation of phase transformation of the material during multiple cycles and accurately predict the phases and the volume change effects, a new methodology is suggested where partial transformation during heating and handling of retained austenite for various cool down scenarios are proposed. This will also handle the volume change effects during transformation. The phase change during heating is based on linear austenitisation rule and the martensite formation during cooling uses Koistinen-Marburger (KM) relation.

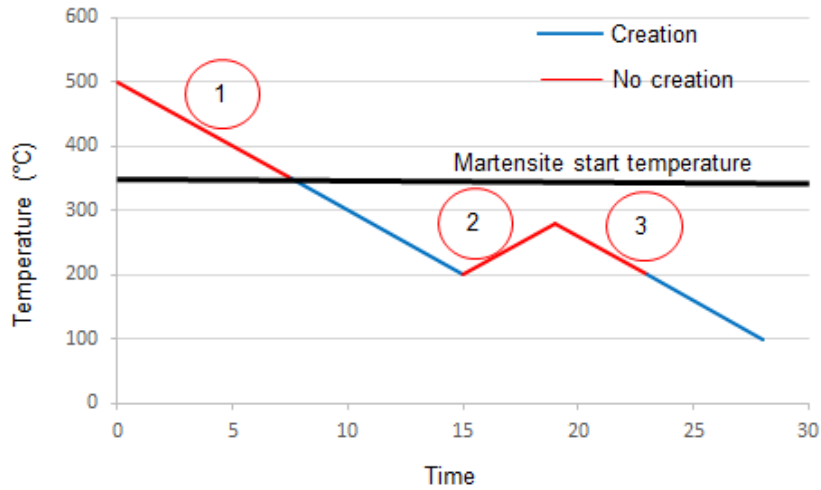


Figure 4: Multi-cycle phase transformation cases

A schematic of the various cases for *creation* and *non-creation* of martensite during cool down is presented in Figure 4. The figure only depicts the cool down cases and the logic of martensite phase formation during multiple thermal cycles. The region depicted 1 indicates the cooling down of material but above martensite start temperature, whereas regions 2 and 3 indicate situations where the temperature of the material point during subsequent thermal cycles, does not go beyond martensite start temperature but is definitely more than the temperature state from previous cycle's cooling stage. In these situations, there will not be any martensite creation. The regions marked blue are those where martensite calculation is undertaken. Any TRIP effects present during the build process are ignored due to lack of any appropriate material data or evidence for such an effect during the build process.

6 Results

Based on the simulation methodology presented in above sections in addition to the material phase transformation modelling, the thermal history in the double-hat profile is predicted which was used to predict the phase evolution, stresses and deformation in the part. Figure 5 shows the equivalent stress distribution predicted in the part on the left side and the flow stress/hardening of the part on the right.

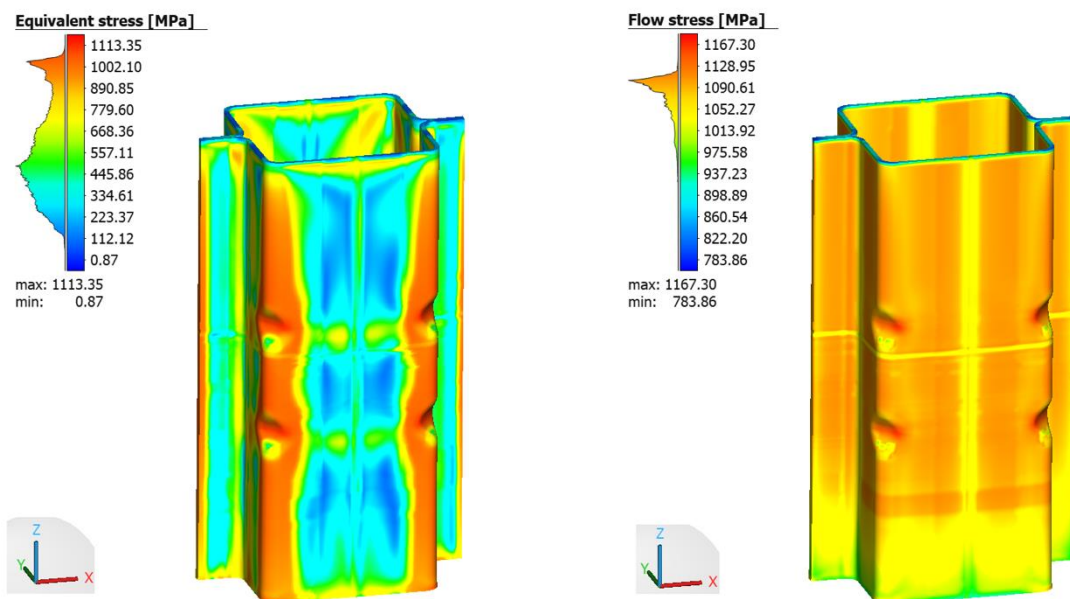


Figure 5: Predicted equivalent stress (left); flow stress in the double-hat specimen (right)

It should be noted that the results are extracted with the baseplate still attached to the part. Results indicate that AM process introduces considerable residual stresses and hardening in the part due to repetitive thermal cycles.

The distribution of martensite phase and total deformation is presented in Figure 6. It can be seen from the phase distribution that the martensite phase is not the same across various regions in the layer. The same is observed in the temperature predictions in the part as depicted in Figure 7 where the temperature predictions are different between layers and also within a certain layer. The analysis has been terminated when the temperature at every integration point reached below 100 °C to save computational time.

The image on the right side in Figure 7 shows the track based deposition of the layer profile from left to right as indicated in Figure 3 (top). It is interesting to note that the temperature in the previously deposited layer is different across various tracks in the same layer, owing to the differences in the deposition and cooling times/sequence within the layer. This shows that with the proposed methodology greater resolution is achieved within a layer. These differences in the cooling times/sequence lead to differences in the predicted martensite fractions within a layer. Since the stresses are calculated as a weighted sum of the individual phase fractions, the hardening and the flow stress values are also different within a layer, thereby providing greater spatial resolution and improved accuracy in the overall performance of simulation.

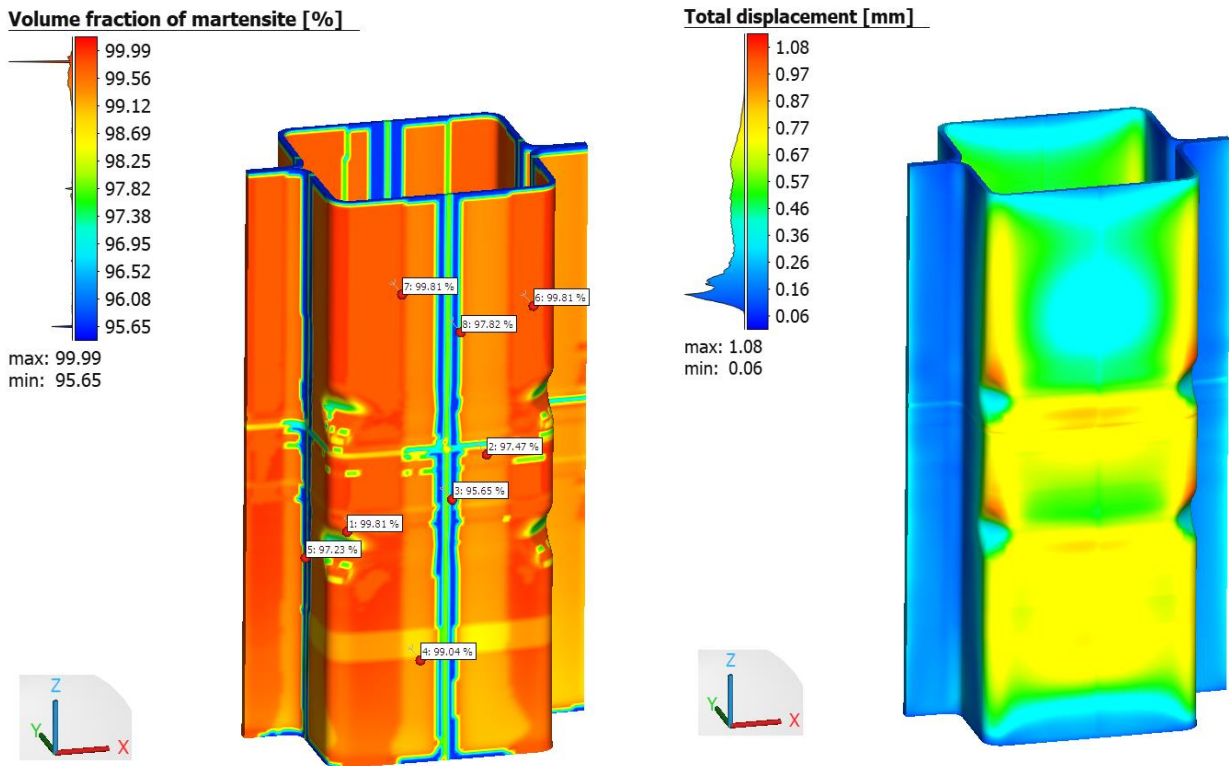


Figure 6: Predicted martensite distribution (left); total deformation in the double-hat specimen (right)

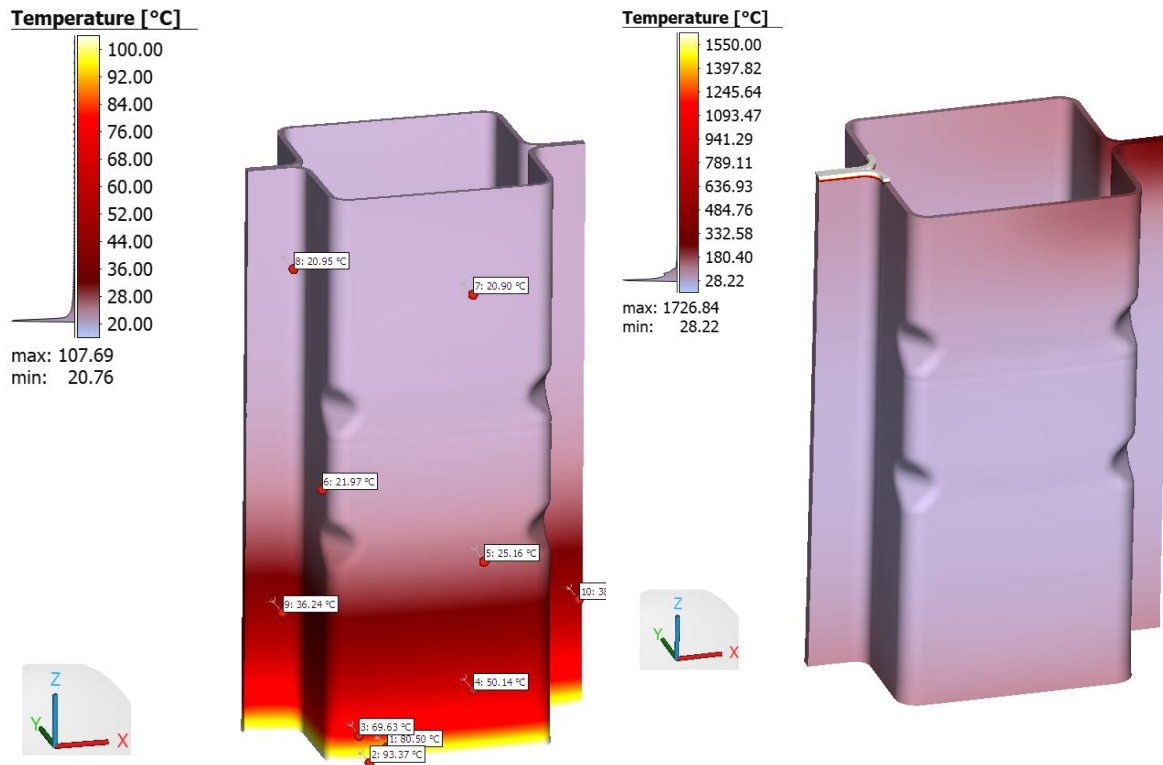


Figure 7: Predicted temperature distribution in the double-hat specimen (left); track based element activation (right)

Conclusions

Based on the simulation approach presented in this paper, it can be concluded that the current methodology provides better details of the actual SLM process by effectively capturing some of the transient nature of process characteristics and material behaviour. Such models can be computationally intensive than that of the layer-wise models prevalent in the literature currently. Nevertheless, the level of detail and resolution can justify such intensity especially in cases of crash components where safety is of paramount importance. Another crucial emphasis is on the consideration of multiple phase transformation cycles in order to capture the right material behaviour in terms of hardening, phase distribution and residual stress/deformation generation. Further work with experimental validation and process chain simulation are necessary.

Acknowledgements

This work was performed within the project „Additive Manufacturing Technologies for Crash loaded structural Components (AM-Crash)“ and supported by the Federal Ministry of Education and Research (BMBF) and by the Polish National Centre for Research and Development (NCBR) under international programme M-ERA.NET 2 Cofund Financial support is gratefully acknowledged.

References

- [1] Chandan, A.; Sahoo, B.; Bansal, G.: Medium Manganese Steel: A Promising Candidate for Automotive Applications. *Steel Tech.* 15 (2001) 2, pp. 60–66.
- [2] Schmitt, J-H.; Thierry I.: New developments of advanced high-strength steels for automotive applications. *C. R. Physique* 19 (2018), pp. 641–656.
- [3] Yusofa, N.S.B.; Sapuana, S.M.; Sultand, M.T.H.; Jawaida, M.; Malequee, M.A.: Design and materials development of automotive crash box: a review. *Ciência & Tecnologia dos Materiais* 29 (2017), pp. 129–144.
- [4] Boreanaz, M. (2018). Development of crash box for automotive application (Doctoral Thesis). The Polytechnic University of Turin.
- [5] The Aluminium Automotive Manual. Version 2013 © European Aluminium Association.
- [6] Gausemeier, J.; Echterhoff, N.; Wall, M.: Thinking ahead the Future of Additive Manufacturing – Innovation Roadmapping of Required Advancements. University of Paderborn 2013.
- [7] Zopp, C.; Schubert, F.; Palm, F.; Lohner, H.; Syassen, F.; Kroll, L: Selective laser melting of a new tailored aluminium alloy (SilmagAl® AISi7Mg0.6) for aerospace industry. In: 2nd International Conference on 3D Printing Technology and Innovations, London, 2018, p. 67, DOI: 10.4172/0976-4860-C1-002
- [8] Laakso, P., et al.: Optimisation and simulation of SLM process for high density H13 tool steep parts. *Physics Procedia.* 83 (2016), pp. 26–35.
- [9] Ghnatios, C.: Reduced order modeling of selective laser melting: from calibration to parametric part distortion. *Int J Mater Form* 14 (2021), pp. 973–986.
- [10] Höfemann M. et al. (2020) Ein niedriglegierter Stahlwerkstoff für die Laseradditive Fertigung – Prozesskette und Eigenschaften. In: Lachmayer R., Rettschlag K., Kaierle S. (eds) *Konstruktion für die Additive Fertigung 2019*. Springer Vieweg, Berlin, Heidelberg. https://doi.org/10.1007/978-3-662-61149-4_3
- [11] Yancheng, Z.; et al.: Macroscopic thermal finite element modeling of additive metal manufacturing by selective laser melting process. *Comput. Methods Appl. Mech. Engrg.*, 331 (2018), pp. 514–535.
- [12] Gu, H.; Wei, C.; Li, L.; et al.: Multi-physics modelling of molten pool development and track formation in multi-track, multi-layer and multi-material selective laser melting. *International Journal of Heat and Mass Transfer* 151 (2020).
- [13] Kiran, A.; Hodek, J.; et al.: Numerical Simulation Development and Computational Optimization for Directed Energy Deposition Additive Manufacturing Process. *Materials* 13 (2020). doi:10.3390/ma13112666